

Journal of Visualized Experiments

A murine model of burn wound reconstructed with an allogeneic skin graft

--Manuscript Draft--

Article Type:	Invited Methods Article - Author Produced Video
Manuscript Number:	JoVE61339R2
Full Title:	A murine model of burn wound reconstructed with an allogeneic skin graft
Section/Category:	JoVE Biology
Keywords:	Wound healing, full thickness burn, skin transplantation, murine allograft, wound reconstruction, in vivo mouse model, cutaneous injury
Corresponding Author:	Nadira Frescaline Ecole Polytechnique Palaiseau, Ile-de-France FRANCE
Corresponding Author's Institution:	Ecole Polytechnique
Corresponding Author E-Mail:	nadira.frescaline@lpp.polytechnique.fr
Order of Authors:	Océane Blaise Constance Duchesne Sébastien Banzet Antoine Rousseau Nadira Frescaline, Ph.D.
Additional Information:	
Question	Response
Please indicate whether this article will be Standard Access or Open Access.	Open Access (US\$3000)

TITLE:

A Murine Model of a Burn Wound Reconstructed with an Allogeneic Skin Graft

AUTHORS AND AFFILIATIONS:

Océane Blaise^{*1,2}, Constance Duchesne^{*1,2}, Sébastien Banzet², Antoine Rousseau¹, Nadira Frescaline^{1,2}

¹Laboratoire de Physique des Plasmas, École Polytechnique, Sorbonne Université, CNRS, Palaiseau, France

²Institut de Recherche Biomédicale des Armées, Clamart, INSERM UMRS-MD, France

*These authors contribute equally

Email addresses of co-authors:

Océane Blaise (oceane.blaise@lpp.polytechnique.fr)

Constance Duchesne (constance.duchesne@lpp.polytechnique.fr)

Sébastien Banzet (sebastien.banzet@inserm.fr)

Antoine Rousseau (antoine.rousseau@lpp.polytechnique.fr)

CORRESPONDING AUTHOR:

Nadira Frescaline(nadira.frescaline@lpp.polytechnique.fr)

KEYWORDS:

Wound healing, full thickness burn, skin transplantation, murine allograft, wound reconstruction, in vivo mouse model, cutaneous injury

SUMMARY:

The aim of this study was to develop a murine model of burn wound healing. A thermal burn was induced on the dorsal skin of mice using a preheated brass template. Burned tissue was debrided and overlaid with a skin graft harvested from the tail of a genetically similar donor mouse.

ABSTRACT:

Trivial superficial wounds heal without complications by primary intention. Deep wounds, such as full thickness burns, heal by secondary intention and require surgical debridement and skin grafting. Successful integration of the donor graft into a recipient wound bed depends on timely recruitment of immune cells, robust angiogenic response and new extracellular matrix formation. The development of novel therapeutic agents, which target some key processes involved in wound healing, are hindered by the lack of reliable preclinical models with optimized objective assessment of wound closure. Here, we describe an inexpensive and reproducible model of experimental full thickness burn wound reconstructed with an allogeneic skin graft. The wound is induced on the dorsum surface of anaesthetized inbred wild type mice from the BALB/C and SKH1-Hrhr backgrounds. The burn is produced using a brass template measuring 10 mm in diameter, which is preheated to 80 °C and delivered at a constant pressure for 20 s. Burn eschar is excised 24 hours after the injury and replaced with a full thickness graft harvested from the tail

of a genetically similar donor mouse. No specialized equipment is required for the procedure and surgical techniques are straightforward to follow. The method may be effortlessly implemented and reproduced in most research settings. Certain limitations are associated with the model. Due to technical difficulties, the harvest of thinner split thickness skin grafts is not possible. The surgical method we describe here allows for the reconstruction of burn wounds using full thickness skin grafts. It may be used to carry out preclinical therapeutic testing.

INTRODUCTION:

Surgical debridement and skin grafting are common clinical practices used in the management of chronic wounds¹, burn wounds², and acute wounds such as traumatic wounds³. Skin grafting refers to the surgical procedure, which involves the removal of healthy skin from one part of the body and transferring it to another. Donor grafts replace the lost tissue and provide a structural scaffold for cellular migration and growth. Following integration into the recipient site, skin grafts replace the lost skin barrier by providing protection from microbial invasion, harmful effects of the external environment and excessive loss of moisture⁴. Successful skin graft integration depends on several factors. These include adequate immune responses in the presence of microbial infections and timely resolution of inflammation, robust angiogenesis at the wound site and establishment of vascular anastomoses between the recipient bed and the donor graft⁵. As the graft begins to degrade, resident dermal cells must be replaced by cells capable of producing new extracellular matrix. At the same time, the epidermal keratinocytes must crawl over the newly produced matrix to form the neo-epidermis and re-epithelialize the wound. It is, therefore, evident that efficient migration of cells from the recipient bed into the donor graft is another determining factor that influences successful graft incorporation. Given the vast number of factors involved in wound healing⁶, which may be impossible to control in the human trials due to ethical limitations, models of pre-clinical experimental skin grafting are necessary. Development of pre-clinical models of burn wound healing and associated skin grafting will be important for understanding of complex mechanisms involved in cutaneous tissue repair and essential for the testing of new therapeutic agents. The in vitro models of wound healing are unable to accurately mimic the complexity of the cutaneous tissue. The in vivo animal models are an indispensable investigative tool in understanding the mechanisms involved in tissue repair.

Several methods of skin grafting technique were developed in rodents to mimic surgical excision and burn wound reconstruction⁷⁻⁹. However, most of the previously described procedures failed to induce a thermal burn injury prior to skin grafting. Instead of the burn wound, a full thickness excisional wound was induced, which was then reconstructed with a full thickness skin allograft⁷. Various anatomical landmarks such as the ear, tail and back have been used for harvesting of the donor skin in rodents^{7,8}. Different graft fixation and stabilization techniques were reported, including a “no suture technique”⁹, sutures⁷ and surgical glue¹⁰⁻¹².

The purpose of this study was to develop a murine model of a full thickness burn wound that would recapitulate the current gold standard approach in burn treatment, which involves nonviable tissue excision and skin grafting. A thermal burn was induced on the dorsum surface of a mouse using a preheated brass template. Burn eschar was excised and replaced with a full thickness graft harvested from the tail of a donor mouse. There are three key advantages to this

experimental model. First, more than one burn wound may be induced on the back of the recipient mouse, and four donor skin grafts may be harvested from a single tail of the donor mouse. This means that several experimental and control treatments may potentially be compared using the same recipient and donor animals. Depending on the desired route of administration, the control treatment may include local or systemic administration of the vehicle or placebo control (e.g., topical application of ointment, subcutaneous, intraperitoneal or intravenous injection of solution). Second, timing of the treatment and the endpoint of the experiment may be controlled. Third, this model depends on the reconstruction of wounds using full thickness grafts harvested from the tail, which are known to have a higher probability for successful incorporation into the donor site compared to the skin harvested from the back¹³. This may be due to the lower number of epidermal Langerhans cells, which play a key role in cutaneous immunobiology, and are associated with the skin graft rejection¹⁴.

The proposed model of wound healing and graft integration may well be applied to transgenic and knockout mice. The use of genetically modified mice will assist in elucidating the roles that certain genes may play during wound repair. Exogenous application of topical wound preparations or subcutaneous administration of therapeutic antibodies at the site of the injury may also be considered.

Due to technical difficulties, split thickness skin grafts consisting of the epidermis and part of the dermis are difficult to obtain in mice. Full thickness skin grafts consisting of the epidermis and full thickness dermis are known to require a well-vascularized wound bed for successful integration. The inability to harvest split thickness skin grafts in mice may be regarded as a limitation of this model. The fixation of the skin graft to the recipient wound bed was achieved via the application of the surgical adhesive glue, which is associated with less trauma and rapid degradation compared to other means of tissue fixation¹⁵. Previous studies have shown that suturing is associated with stronger tissue fixation than the surgical glue at 24 h after the surgical procedure¹⁵, which may be considered as a disadvantage of the procedure. However, at later timepoints, the biomechanical strength of wounds treated with a surgical adhesive becomes comparable to sutures¹⁵ and better than staple fixation¹⁶. Following tissue fixation with the surgical glue, wounds must be covered with a wound dressing. Although wounds on the dorsal surface of the mouse are difficult for the animal to reach, the wound dressing, on the other hand, is easy for the animal to manipulate and remove. Frequent wound dressing changes may be warranted.

Anesthesia-induced hypothermia in small rodents is a well-documented phenomenon¹⁷. Hypothermia is a side effect of this procedure, which causes complications, and potentially compromises both animal health and data quality. Therefore, this method warrants the implementation of temperature management strategies, especially if hairless SKH1-Hrhr are used.

The most significant limitation of using mice to mimic human wound closure is the difference between the skin anatomy and physiology. Mouse wounds heal mostly via contraction, whereas human wounds heal through granulation tissue formation and re-epithelialization¹⁸. To account

for this discrepancy, the current model may be modified and used in combination with a splinting ring tightly adhered around the wound to prevent skin contraction¹⁹. Given some advantages and disadvantages of this in vivo protocol, this model could serve as a tool to study certain processes involved in wound healing that are impossible to study in vitro.

PROTOCOL:

All experiments were approved by the French Department of Higher Education and Research (Study Number: 122162017111616517670v2 and DAP180012). All mice were single-housed upon arrival in plastic cages and were allowed a 7-day acclimatization period prior to the study. The animal room was maintained at a 12/12 h light/dark cycle (lights on at 07:00). Food and tap water were provided ad libitum. BALB/c and SKH1-Hrhr mice were fed traditional wheat/soy-based diet. Sawdust bedding was provided along with nesting material.

1. Equipment preparation

1.1 Prepare a burning device for the procedure and set it to 80 °C using the temperature controller (**Figure 1A**). Verify the temperature of the brass template (**Figure 1B,C**) using the infrared thermal imaging camera.

1.2 Ensure that the digital manometer is operating correctly.

1.3 Cover the stage with a surgical drape and adjust the height of the table (**Figure 1A**).

2. Pre-operative and intra-operative animal care

2.1 Acquire BALB/c and SKH1-Hrhr mice, 6-8 weeks of age.

2.2 Add paracetamol suspension at 3 mg/mL to drinking water and supply 12 hours before and up to 72 hours after the procedure.

2.3 Using a 1 mL syringe and a 26 G needle, administer buprenorphine subcutaneously at 0.05 µg/g 30 min before the procedure and every 6 hours for the first 72 hours after the procedure.

2.4 Using a 1 mL syringe and a 26 G needle, administer lidocaine to the dorsum of the mouse and 2-3 mm distal to the area of the burn wound. Inject lidocaine at 0.05 µg/g subcutaneously 15 min before the induction of the burn wound.

2.5 Anesthetize mice using an intraperitoneal injection of xylazine at 10 mg/kg and ketamine 100 mg/kg. Use a 1 mL syringe and a 26 G needle to administer the injection.

2.6 Critical step: Place the anaesthetized mouse on a heated pad and keep the mouse warm to prevent hypothermia for the first 30 minutes after the induction of anesthesia and for at least 15 minutes after the recovery from anesthesia. In addition to the heated pad, other modalities

including heat lamps, circulating warm liquids or air, and pre-warmed heat reservoirs may be used to regulate the body temperature.

2.7 Apply lubrication gel on the eyes of the mouse to prevent dehydration of the cornea.

2.8 Use the toe pinch withdrawal reflex to assess the depth of anesthesia.

2.9 Using a 1 mL syringe and a 26 G needle administer 200 μ L of Lactated Ringer's Solution supplemented with 5% dextrose. Administer fluid replacement subcutaneously immediately after the induction of anesthesia and 6 hours after the procedure to prevent dehydration.

3 Full thickness burn wound induction

3.1 Shave the anaesthetized mouse with the hair clippers.

3.2 Apply depilating cream on the dorsum surface of the mouse for 1 minute. Wipe off the cream using some sterile gauze and clean the area with a piece of damp gauze. Blot the skin with some gauze until dry.

3.3 Place the mouse on the stage covered with a surgical drape and move the stage upward closer to the preheated brass template.

3.4 Apply the circular brass template on the back of the mouse (80 °C for 20 s) using constant pressure of 0.15 N (**Figure 2**).

3.5 **Critical step:** Immediately after the burn induction, place the anaesthetized animal on the heated pad to prevent hypothermia and keep the mouse warm during and after the procedure. Once recovered from anesthesia, return the mouse back to the cage.

3.6 **Critical step:** Provide a mashed diet on the cage floor for the first 72 hours after the surgical procedure. Mice are sometimes reluctant to reach up to a sipper tube to drink water after a burn wound injury.

4 Harvesting of the donor graft

4.1 Make a longitudinal incision with a scalpel in the upper part of the tail of the donor mouse and gently remove the skin using surgical forceps.

4.2 Place the tail skin into a sterile Petri dish filled with 10 mL of sterile 0.9% saline solution. Use a ruler to measure out individual grafts and cut the tail skin into pieces, each measuring 15 mm, using a scalpel.

4.3 Once prepared, keep the skin grafts in 0.9% saline solution at 4 °C for up to 2 hours.

5 Surgical excision and skin grafting

5.1 Twenty-four hours after the burn induction, prepare the mouse for anesthesia by inhalation of isoflurane. Place the mouse into the induction chamber and induce anesthesia using 5% isoflurane in 100% oxygen at a flow rate of 4 L/min. To maintain anesthesia during surgery, use 2% isoflurane at 2 L/min.

5.2 Place a surgical drape on the mouse and cut out a window to expose the surgical field. Using the aseptic technique, swab the wound first with povidone-iodine and then with 70% alcohol.

5.3 Gently pick up the burned tissue with a pair of surgical tweezers and excise all necrotic and nonviable tissue with sterile surgical scissors and tweezers. Remove the panniculus carnosus layer of the hypodermis to create a stable recipient bed.

5.4 Place the skin graft on the freshly prepared wound bed. Gently pull the surrounding skin toward the skin graft using surgical tweezers. Apply some surgical adhesive to attach the graft to the wound bed and gently press to align the skin edges. **Critical step:** The size of the wound bed must be slight larger than the size of the skin graft to ensure successful engraftment.

5.5 Allow the mouse to recover from anesthesia. **Critical step:** Place the mouse on a heated pad. Keep the mouse warm during and after the procedure to prevent hypothermia.

5.6 Apply inert paraffin gauze dressing and adhesive secondary dressing over the grafted wound.

5.7 Place the mouse into an individual cage. **Critical step:** Provide some mashed diet on the cage floor for the first 72 hours after the surgical procedure and monitor daily.

5.8 Provide toys and enrich the environment.

6 Digital imaging and post-mortem wound collection

6.1 Photograph wounds with a digital camera by placing a ruler next to the wound (**Figure 3**).

6.2 At the end point of the experiment, euthanize animals by exposure to carbon dioxide and cervical dislocation. **Critical step:** Excessive pulling action of the skin during the cervical dislocation may damage the graft.

6.3 At post-mortem, surgically excise the dorsal burn wounds to the fascia using scissors. Bisect wounds. Fix half in 10% buffered formalin and process for histology and immunohistochemistry. Fast freeze the other half in liquid nitrogen for RNA extraction and protein quantitation and keep at -80 °C.

7 Skin histology, immunohistochemistry and collagen visualization

7.1 Embed samples of skin into paraffin, cut to 4 μm sections and place onto positively charged slides.

7.2 Use slides stained with hematoxylin and eosin to evaluate the rate of re-epithelialization (% of the original wound). The area of the wound that is covered with neo-epidermis may be expressed as a percentage of the entire wound (**Figure 4**). Use a digital microscope application and ImageJ software to perform the microscopic analysis of the sections.

7.3 Use histological sections (4 μm thickness) prepared from formalin-fixed and paraffin-embedded tissue and subject them to immunohistochemistry.

7.4 To assess collagen I and fibronectin expression in wounds, apply primary antibodies and incubate for 1 h. Detection may be performed by species-specific horseradish peroxidase (HRP) or alkaline phosphatase (AP)-conjugated secondary antibodies.

7.5 React sections with either: (i) HRP,3,3'-diaminobenzidine (DAB) or (ii) AP, Bond Polymer Refine Red (Table of Materials), which yields a bright red color (**Figure 5**). Scan the sections using an instrument and analyze with the digital microscope application and ImageJ.

7.6 To enable histological assessment of collagen deposition, perform trichrome staining on histological sections using a commercial kit.

7.7 For collagen fiber visualization, use multiphoton microscopy and second harmonic generation technique (**Figure 5**). Use a multiphoton microscope for tissue imaging as previously described²⁰. Use a Ti:Sapphire laser with a center wavelength at 810 nm as the laser source for generating second harmonic and two-photon excited fluorescence signals (TPEF).

7.8 Use a laser beam equipped with a 25x/0.95 W objective to collect and excite second harmonic generation (SHG) and TPEF. Detect signals as described previously²¹ by NDD PMT detectors. Use software for laser scanning control and image acquisition.

REPRESENTATIVE RESULTS:

The results demonstrate that the protocol developed is a straightforward method, which permits the induction of a full thickness burn wound in mice. Burns are induced using a preheated brass template (**Figure 1A-C**). The burned area appears as a circular wound with a white eschar and a hyperemic zone. The size of the burn wound is slightly larger at 24 hours after the burn injury as a result of the well-described phenomenon known as the burn injury progression, which is possibly due to acute inflammation²². After excision, burn wounds are reconstructed using allogeneic skin graft (**Figure 3**). On day 7 after the burn injury, wounds become vascularized⁵, which is an indication of successful engraftment. Epidermal keratinocytes migrate from the adjacent recipient skin in the effort to close the wound and bridge the gap between the two edges of the wounds. Microscopic analysis of H and E stained section of wounds revealed that

the length of the neo-epidermis becomes significantly longer on day 7 after burn injury compared to day 3 after burn injury (**Figure 4B**). Prior to performing a large study, it is highly recommended that researchers complete a pilot study, which enables the exploration of a novel intervention, assessment of feasibility, identification of modifications to the method to ensure reproducibility. Statistically significant effects are difficult to detect in smaller samples, whereas increasing the sample size is one way to boost the statistical power of a test. For example, to detect a statistically significant difference ($p < 0.05$) in the rate of wound re-epithelialization (**Figure 4**) between groups, the sample size should be between six and eight mice per group. All experiments should be repeated at least twice. As matrix producing cells, such as fibroblasts, migrate from the recipient tissue into the graft, key components of the extracellular matrix, including collagen I and fibronectin become highly expressed in the newly formed matrix (**Figure 5**).

Figure 1: Burning device setup. (A) Placement and set-up of the burning device. The burning device is connected to the temperature controller and is attached to the digital monometer to enable the monitoring of pressure. The burning device is suspended above an adjustable stage – flat surface onto which mice are placed for the induction of burn. (B-C) A close up image of the brass template used to induce wound burns. (C) The diameter of the brass template is 1 cm.

Figure 2: Schematic illustration of the different steps required to reproduce the experimental model described in this article. There are three main steps to the procedure: (i) induction of the burn wound using a preheated brass template; (ii) surgical excision of the non-viable necrotic tissue at 24 hours after the burn injury; (iii) surgical wound reconstruction using a full thickness allogeneic skin graft harvested from a donor mouse.

Figure 3: The macroscopic view of reconstructed mouse burn wounds. Representative digital images of burn wounds reconstructed with allogeneic skin grafts on days 0, 1, 3 and 7 after burn injury. The ruler on images is in millimeters.

Figure 4: Microscopic appearance of wounds at 3 and 7 days after burn injury. H&E-stained sections of wounds 3 and 7 days after burn injury. The length of neo-epidermis (dotted line) is significantly increased in (A) day 3 wounds compared to (B) day 7 wounds. In (A) and (B), the scale bar is 100 μm . (C) Graphical representation of the percentage of wound re-epithelialization. This was evaluated by measuring the length of neo-epidermis at day 3 and 7 post-burn injury and expressed as a percentage of the whole wound length. Results represent mean \pm S.E.M. ($n = 6$ mice in day 3 group; $n = 6$ mice in day 7 group, $*p < 0.05$; Student's t-test).

Figure 5: Assessment of the extracellular matrix and collagen I visualization. Representative images of immunohistochemistry analysis on day 7 mouse wounds stained for (A) collagen and (B) fibronectin. Note intense red staining in elongated spindle-shaped collagen I-positive cells. Note brown staining in fibronectin-positive cells in the dermis of day 7 wounds. Scale bar = 50 μm in all images. In (A) and (B), e denotes epidermis and d denotes dermis. (C) Visualization of collagen fibers and histological assessment of collagen deposition. (D) Representative TPEF/SHG collagen image of day 7 mouse wounds. Simultaneous TPEF/SHG acquisition using circular polarization and SHG signals were selectively processed to obtain a binary distribution of SHG

after applying a threshold. TPEF images (green) and SHG images (white) were pseudo-colored and overlaid. Scale bar = 50 μ m.

DISCUSSION:

According to the thickness classification of burn injury²³, full thickness burns are characterized by evident involvement of the whole thickness of the skin and certain portion of the subcutaneous tissue. This type of wound can heal only by contraction or with skin grafting². An inherent limitation of the method described in this article is that only full thickness grafts, as opposed to the split thickness grafts, which are often used in the clinical setting, were harvested from the tail of a mouse. This was due to the technical difficulty, as the mouse skin is too thin to obtain split thickness grafts. It must be pointed out that full thickness grafts require a well vascularized wound bed, whereas split thickness skin grafts are able to survive at donor sites with less vascularity²⁴. Previous studies showed that a burn wound induced on the back of the mouse was associated with a robust formation of new vasculature⁵. This suggests that a well vascularized area, such as the dorsum of the mouse, could be considered as the anatomical landmark for the induction of burn wounds.

Burn wound depth is an important factor to consider. The depth of the burn wound must be consistent between individual mice. The reproducibility of the burn wound depth depends on the temperature of the brass template, pressure and duration of the heat exposure. The burn wound depth must be verified histologically. It is important to keep in mind that excessive pressure or prolonged exposure of the skin to the preheated brass template may injure the underlying tissue. The tissue surrounding the vertebral column, including the components of the central and peripheral nervous system, are sensitive to heat, and if damaged may result in hind leg paralysis.

Although no postoperative mortality was directly associated with the surgical procedure, a small number of hairless SKH1-Hrhr mice, which are especially sensitive to cold, developed hypothermia and failed to recover after the general anaesthesia. Therefore, supplementary heat must be provided during all aesthetic events and constant surveillance is required while the mouse is anaesthetized.

The method described in this study was not associated with the surgical site infection. However, aseptic technique must be used to prevent the transfer of microorganisms into the surgical wound during the perioperative period. Inoculation of the wound with bioluminescent or fluorescent microorganisms may be incorporated into the procedure. This technique may be useful in studying infectious organisms and their pathogenesis²⁵. For example, exogenous addition or injection of bioluminescent bacteria, may permit the monitoring of the microbial burden using the in vivo whole animal imaging²⁵. Given that mouse hair is known to interfere with the in vivo whole animal fluorescence and bioluminescence imaging, hairless SKH1-Hrhr mice are ideal hosts for the studies involving fluorescent or bioluminescent reporters.

Wound tissue samples may be collected at different time points and processed for histological and immunohistochemical analysis. Protein and RNA may be isolated from the skin biopsy and

molecular biology techniques may be used to assess the expression of key molecules involved in wound healing.

In the present study, we described an experimental model of burn wound healing and allogeneic skin engraftment. This procedure can be modified and serve as a model for preclinical studies.

ACKNOWLEDGMENTS:

This work was supported by La Direction Générale de L'Armement, l'Agence de l'Innovation de Défense and École Polytechnique. We thank our colleague Mr Yann Plantier from École Polytechnique who provided insight and expertise that greatly assisted the production of the video file. The authors thank Mr Benoit Peuteman and Ms Charlotte Auriau from INSERM Lavoisier (SEIVIL) US 33, Hôpital Paul Brousse, Villejuif for their animal well-being and care expertise provided during the course of this project.

DISCLOSURES:

The authors declare that they have no competing financial interests.

REFERENCES

- 1 Shakir, S. et al. Indications and Limitations of Bilayer Wound Matrix-Based Lower Extremity Reconstruction: A Multidisciplinary Case-Control Study of 191 Wounds. *Plastic and Reconstructive Surgery* (2019).
- 2 Greenhalgh, D. G. Management of Burns. *New England Journal of Medicine*. **380** (24), 2349-2359 (2019).
- 3 Bosse, M. J. et al. An analysis of outcomes of reconstruction or amputation after leg-threatening injuries. *New England Journal of Medicine*. **347** (24), 1924-1931 (2002).
- 4 Braza, M. E., Fahrenkopf, M. P. in *StatPearls* (2019).
- 5 Duchesne, C., Banzet, S., Lataillade, J. J., Rousseau, A., Frescaline, N. Cold atmospheric plasma modulates endothelial nitric oxide synthase signalling and enhances burn wound neovascularisation. *Journal of Pathology*. **249** (3), 368-380 (2019).
- 6 Eming, S. A., Martin, P., Tomic-Canic, M. Wound repair and regeneration: mechanisms, signaling, and translation. *Science Translational Medicine*. **6** (265), 265sr266 (2014).
- 7 Pakyari, M. et al. Local Expression of Indoleamine 2,3, Dioxygenase Prolongs Allogenic Skin Graft Take in a Mouse Model. *Advances in Wound Care (New Rochelle)*. **8** (2), 58-70 (2019).
- 8 Pakyari, M. et al. A new method for skin grafting in murine model. *Wound Repair and Regeneration*. **24** (4), 695-704 (2016).
- 9 McFarland, H. I., Rosenberg, A. S. Skin allograft rejection. *Current Protocols in Immunology*. **Chapter 4**, Unit 4 4 (2009).
- 10 Cristobal, L. et al. Local Growth Hormone Therapy for Pressure Ulcer Healing on a Human Skin Mouse Model. *International Journal of Molecular Sciences*. **20** (17) (2019).
- 11 Melican, K., Aubey, F., Dumenil, G. Humanized mouse model to study bacterial infections targeting the microvasculature. *Journal of Visualized Experiments* (86) (2014).
- 12 Racki, W. J. et al. NOD-scid IL2rgamma(null) mouse model of human skin transplantation and allograft rejection. *Transplantation*. **89** (5), 527-536 (2010).
- 13 Larsen, C. P. et al. Migration and maturation of Langerhans cells in skin transplants and

explants. *Journal of Experimental Medicine*. **172** (5), 1483-1493 (1990).

14 Leonard, D. A., Kurtz, J. M., Cetrulo, C. L., Jr. Vascularized composite allotransplantation: towards tolerance and the importance of skin-specific immunobiology. *Current Opinion in Organ Transplantation*. **18** (6), 645-651 (2013).

15 Stoikes, N. et al. Biomechanical evaluation of fixation properties of fibrin glue for ventral incisional hernia repair. *Hernia: The Journal of Hernias and Abdominal Wall Surgery*. **19** (1), 161-166 (2015).

16 Foster, K. et al. Efficacy and safety of a fibrin sealant for adherence of autologous skin grafts to burn wounds: results of a phase 3 clinical study. *Journal of Burn Care & Research*. **29** (2), 293-303 (2008).

17 Caro, A. C., Hankenson, F. C., Marx, J. O. Comparison of thermoregulatory devices used during anesthesia of C57BL/6 mice and correlations between body temperature and physiologic parameters. *Journal of the American Association for Laboratory Animal Science*. **52** (5), 577-583 (2013).

18 Grada, A., Mervis, J., Falanga, V. Research Techniques Made Simple: Animal Models of Wound Healing. *Journal of Investigative Dermatology*. **138** (10), 2095-2105 e2091 (2018).

19 Wang, X., Ge, J., Tredget, E. E., Wu, Y. The mouse excisional wound splinting model, including applications for stem cell transplantation. *Nature Protocols*. **8** (2), 302-309 (2013).

20 Ruzehaji, N. et al. Pan PPAR agonist IVA337 is effective in prevention and treatment of experimental skin fibrosis. *Annals of the Rheumatic Diseases*. **75** (12), 2175-2183 (2016).

21 Ruzehaji, N. et al. Combined effect of genetic background and gender in a mouse model of bleomycin-induced skin fibrosis. *Arthritis Research & Therapy*. **17** 145 (2015).

22 Singer, A. J., Boyce, S. T. Burn Wound Healing and Tissue Engineering. *Journal of Burn Care & Research*. **38** (3), e605-e613 (2017).

23 Shakespeare, P. Burn wound healing and skin substitutes. *Burns*. **27** (5), 517-522 (2001).

24 Sun, B. K., Siprashvili, Z., Khavari, P. A. Advances in skin grafting and treatment of cutaneous wounds. *Science*. **346** (6212), 941-945 (2014).

25 Miller, R. J. et al. Development of a *Staphylococcus aureus* reporter strain with click beetle red luciferase for enhanced in vivo imaging of experimental bacteremia and mixed infections. *Scientific Reports*. **9** (1), 16663 (2019).

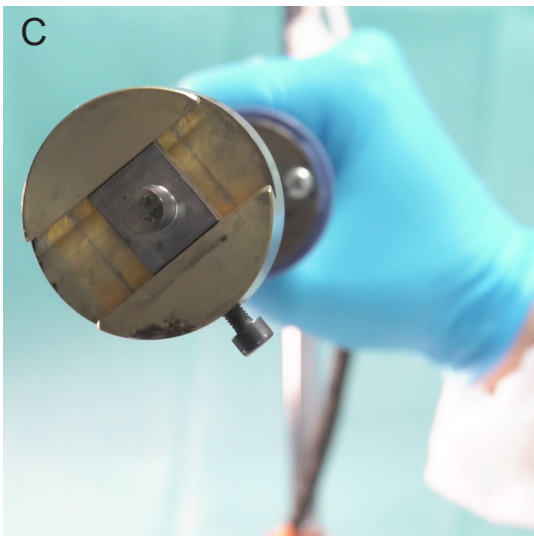
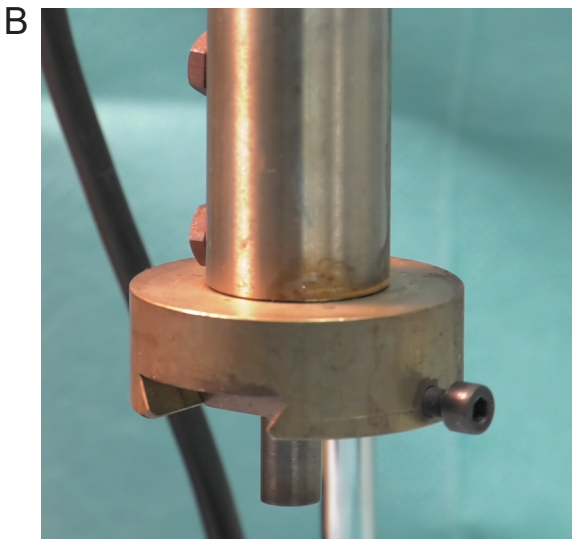
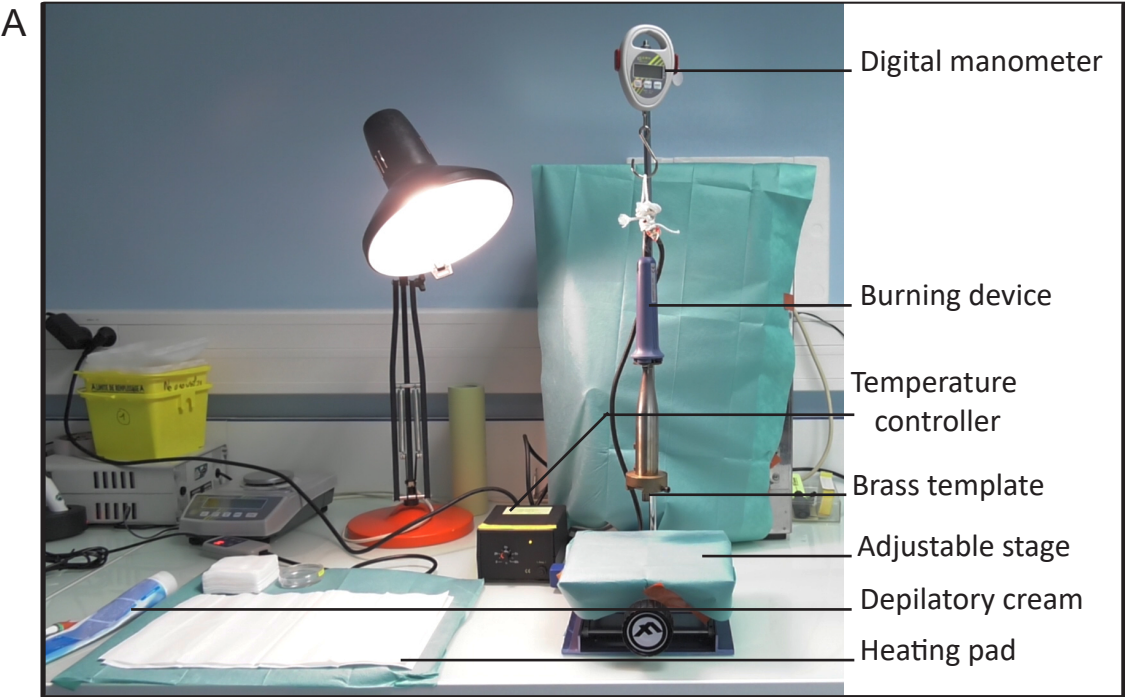
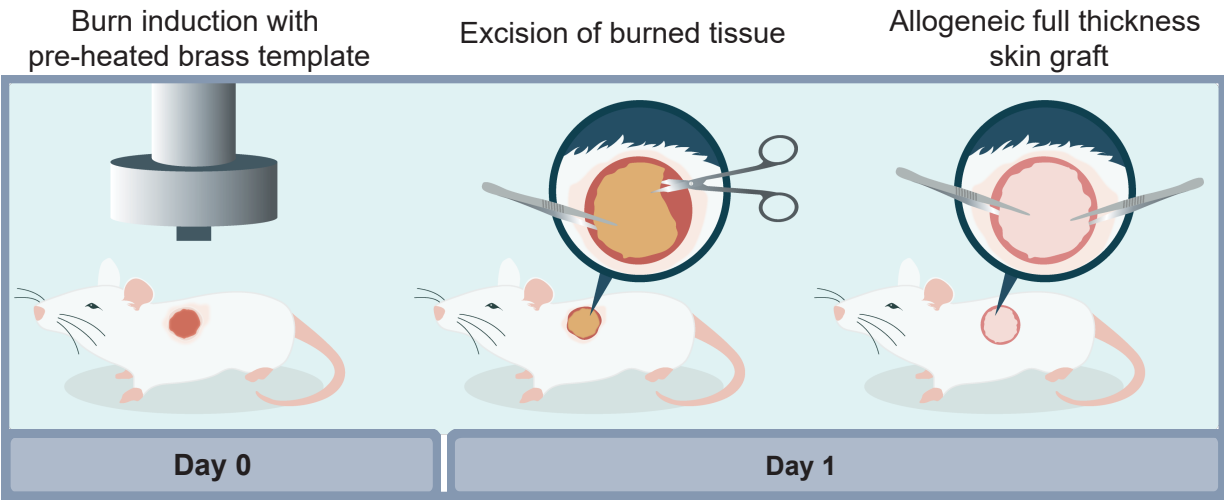
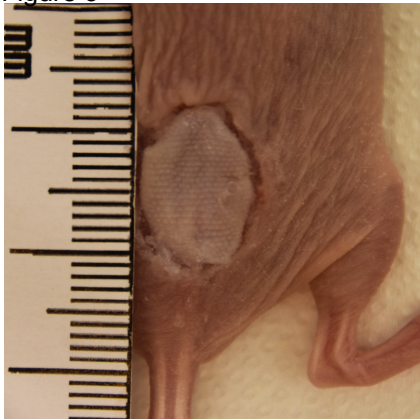
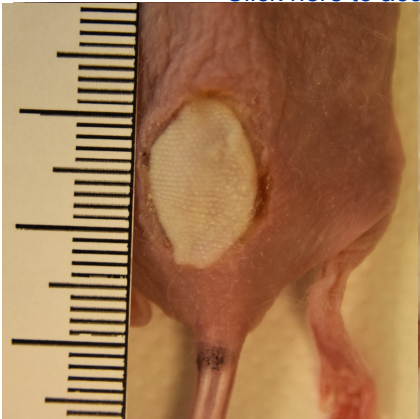


Figure 2

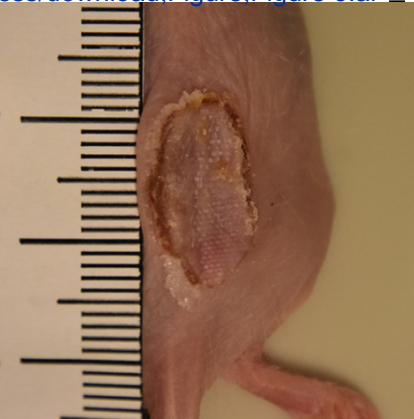




Day 1



Day 3



Day 7

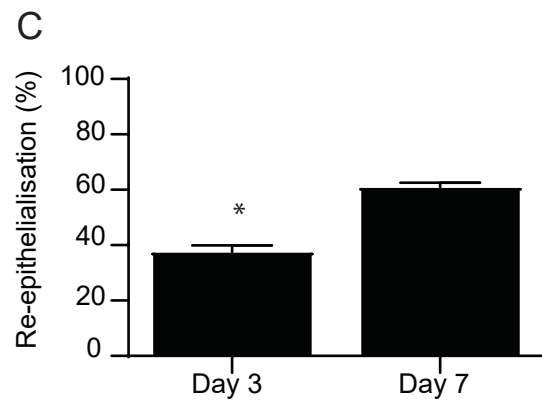
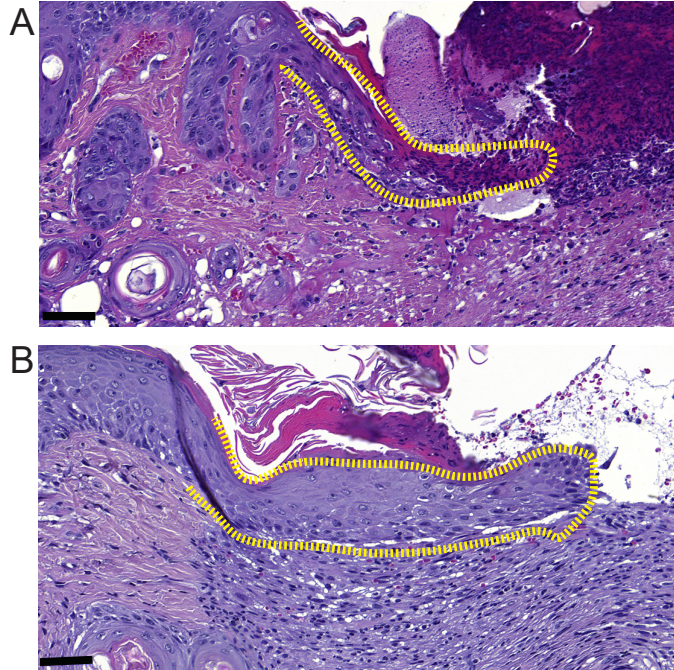
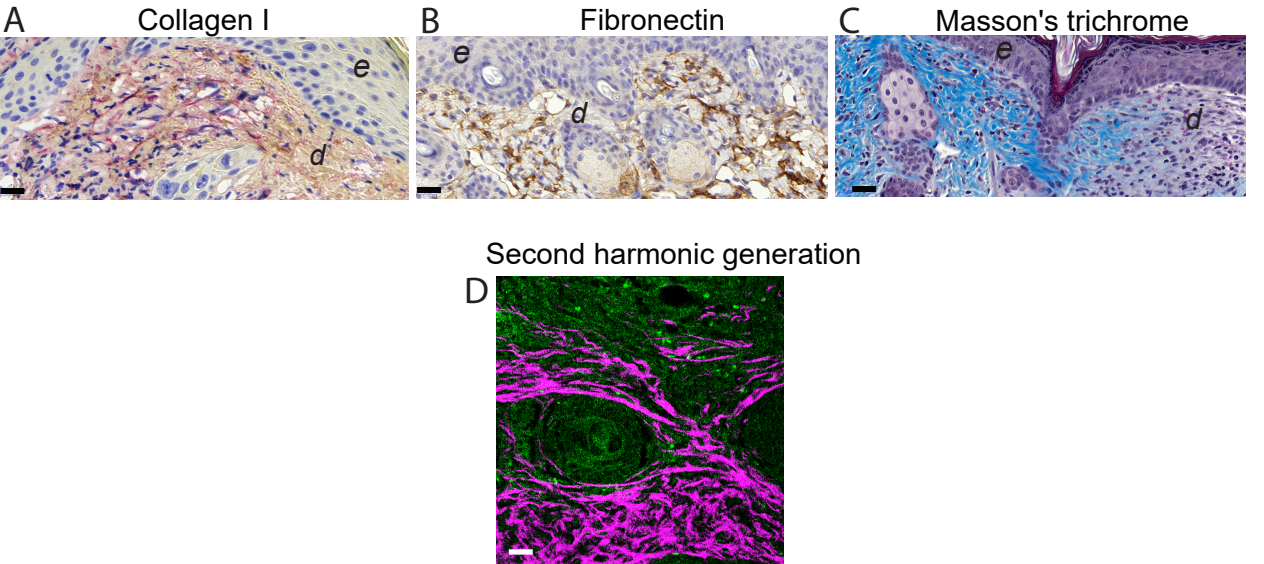


Figure 5

[Click here to access/download;Figure;Figure 5.ai](#) 



Name of Material/Equipment	Company	Catalog Number	Comments/Description
1 ml syringue	Terumo	SS + 01T1	
26 G needle	Terumo Agani	NN-2613R	1/2" - 0,45 X 12mm
96X21 mm Petri Dish	Dutscher	193199	
Animal Weighing scale	Kern	EMB 5.2K5	
BALB/c mouse	Janvier labs	BALB/cAnNRj	6-weeks old
Biopsy foam pads 30.2X25.4X2mm	Simport	M476-1	
Bond polymer Refine Red	Leica Biosystems	DS9390	
Brass block	BVG	custom-designed	Circular 10 mm in diameter
Buprenorphine (BUPRECARE)	Axience	FR/V/6328396 3/2011	administered subcutaneously at a dose of 0.05 µg/ g
Burning apparatus Kausistar 400	TraçaMatrix	34010	
CaseViewer	3DHISTECH Ltd.		3Dhistech, Budapest, Hungary
Collagen I antibody	Abcam	ab34710	Recommanded concentration 1:50; 1:200
D-(+)- glucose (Dextrose)	Sigma Aldrich	G-8769-100 ml	
DAB	Leica Biosystems	AR9432	
Digital camera	NIKON	D3400	objective: SIGMA 18-250mm F3.5-6.3 DC MACRO C45
Depilating cream	Veet		
Disposable scalpels	Swann Morton	6601	
DPBS	PAN biotech	P04-36300	
Ethanol absolute	VWR chemicals	20821.310	
Fibronectin antibody	Abcam	ab23750	Recommanded dilution 1:1000
Filter 0.22µm	Sartorius	16532	
Fine Scissors	F.S.T.	14094-11	
Forceps Dumont	F.S.T.	11295-10	
Hair clippers	AESCU LAP	B00VAQ4KUY (ISIS)	
Heating pad	Petelevage	120070	
Isofluorane	Piramal healthcare	FR/V/03248850/2011	

Ketamine	Imalgene	FR/V/0167433 4/1992	surgical anesthetic, administered intraperitoneally at a dose of 100mg/kg
Lactated Ringers solution	Flee-Flex	1506443	
Lamina multilabel slide scanner	Perkin Elmer		
LAS software	Leica		version 2.7.3
Leica Bond III	Leica Biosystem	1757	
Leukosilk dressing	BSN medical	72669-01	
Lidocaine	Aguettant	N01BB02	local analgesic, administered subcutaneously at a dose of 0.05 µg/g
Manometer	Kern	HDB-5K5	
Masson Trichrome Staining kit	Sigma-Aldrich	HT15-1KT	
Micromesh Biopsy cassettes	Simport	M507	
Multiphoton inverted stand Leica SP5 microscope	Leica microsystems	DM500	Scanner 8000Hz NDD PMT detectors
Non adhering dressing Adaptic	Systagenix	A6222	12.7cm X 22.9 cm
Ocrygel	Tvm France	3700454505621	
Paracetamol 300mg	Dolliprane	Liquiz	
Paraformaldehyde 4%	VWR chemicals	1169945	
Povidone-iodine	MEDA pharma	D08AG02	diluted to 1:2
SKH1-Hrhr mouse	Charles river	686SKH1-HR	6-weeks old
Slides	Thermoscientific	AGAA000080	
Surgical adhesive	BSN medical	9927	
Sterile Gauze	Hartmann	418545/9	10 X 10 cm
Sterile water	Versylene Fresenius	B230521	
Surgical drape	Hartmann	2775161	
Ti:Sapphire ChameleonUltra	Coherent	DS 16-02-16 F	690-1040 nm
Thermal imaging Camera	Testo	Testo 868	

Xylazine (Rompum 2%)	Bayer	FR/V/ 8146715 2/1980	surgical anesthetic, administered intraperitoneally at a dose of 10 mg/kg
----------------------	-------	----------------------	---

Response to reviewer's comments

Manuscript title: *A murine model of burn wound reconstructed with an allogeneic skin graft*

Authors: Océane Blaise, Constance Duchesne, Sébastien Banzet, Antoine Rousseau, Nadira Frescaline

Editorial comments to the author:

Audio, Editing, & Pacing

@02:53 Consider eliminating this shot (with the lifting of the burn device) and just using the next one @02:55.

@02:55 After "infrared thermal imaging camera", there is a stray audio clip of a gasping breath that should be trimmed out. Consider doing a fine-pass on the audio clips to eliminate these extra breaths.

Author's response to the editorial comments: We would like to thank the editor for the thoughtful comments and efforts towards improving our video. All of the comment have been taken into account. The revised version of the video has been upload.



1 Alewife Center #200
Cambridge, MA 02140
tel. 617.945.9051
www.jove.com

ARTICLE AND VIDEO LICENSE AGREEMENT

Title of Article:

A murine model of full thickness burn wound reconstructed with an allogeneic skin graft

Author(s):

Blaise, O., Duchesne, C., Banzet, S., Rousseau, A., Frescaline, N.

Item 1: The Author elects to have the Materials be made available (as described at <http://www.jove.com/publish>) via:

☐

Standard Access

☒

Open Access

Item 2: Please select one of the following items:

☒

The Author is **NOT** a United States government employee.

☐

The Author is a United States government employee and the Materials were prepared in the course of his or her duties as a United States government employee.

ARTICLE AND VIDEO LICENSE AGREEMENT

1. **Defined Terms.** As used in this Article and Video License Agreement, the following terms shall have the following meanings: “**Agreement**” means this Article and Video License Agreement; “**Article**” means the article specified on the last page of this Agreement, including any associated materials such as texts, figures, tables, artwork, abstracts, or summaries contained therein; “**Author**” means the author who is a signatory to this Agreement; “**Collective Work**” means a work, such as a periodical issue, anthology or encyclopedia, in which the Materials in their entirety in unmodified form, along with a number of other contributions, constituting separate and independent works in themselves, are assembled into a collective whole; “**CRC License**” means the Creative Commons Attribution-Non Commercial-No Derivs 3.0 Unported Agreement, the terms and conditions of which can be found at: <http://creativecommons.org/licenses/by-nc-nd/3.0/legalcode>; “**Derivative Work**” means a work based upon the Materials or upon the Materials and other pre-existing works, such as a translation, musical arrangement, dramatization, fictionalization, motion picture version, sound recording, art reproduction, abridgment, condensation, or any other form in which the Materials may be recast, transformed, or adapted; “**Institution**” means the institution, listed on the last page of this Agreement, by which the Author was employed at the time of the creation of the Materials; “**JoVE**” means MyLove Corporation, a Massachusetts corporation and the publisher of The Journal of Visualized Experiments; “**Materials**” means the Article and / or the Video; “**Parties**” means the Author and JoVE; “**Video**” means any video(s) made by the Author, alone or in conjunction with any other parties, or by JoVE or its affiliates or agents, individually or in collaboration with the Author or any other parties, incorporating all or any portion

of the Article, and in which the Author may or may not appear.

2. **Background.** The Author, who is the author of the Article, in order to ensure the dissemination and protection of the Article, desires to have the JoVE publish the Article and create and transmit videos based on the Article. In furtherance of such goals, the Parties desire to memorialize in this Agreement the respective rights of each Party in and to the Article and the Video.

3. **Grant of Rights in Article.** In consideration of JoVE agreeing to publish the Article, the Author hereby grants to JoVE, subject to **Sections 4 and 7** below, the exclusive, royalty-free, perpetual (for the full term of copyright in the Article, including any extensions thereto) license (a) to publish, reproduce, distribute, display and store the Article in all forms, formats and media whether now known or hereafter developed (including without limitation in print, digital and electronic form) throughout the world, (b) to translate the Article into other languages, create adaptations, summaries or extracts of the Article or other Derivative Works (including, without limitation, the Video) or Collective Works based on all or any portion of the Article and exercise all of the rights set forth in (a) above in such translations, adaptations, summaries, extracts, Derivative Works or Collective Works and (c) to license others to do any or all of the above. The foregoing rights may be exercised in all media and formats, whether now known or hereafter devised, and include the right to make such modifications as are technically necessary to exercise the rights in other media and formats. If the “Open Access” box has been checked in **Item 1** above, JoVE and the Author hereby grant to the public all such rights in the Article as provided in, but subject to all limitations and requirements set forth in, the CRC License.